

Low Energy Magnetic Radiation (LEMAR) of Warm Nuclei

S.Frauendorf*

*University Notre Dame,
Notre Dame, IN 46556, USA
E-mail: sfrauend@nd.edu

B. A. Brown

*National Superconducting Cyclotron Laboratory and Department of Physics and
Astronomy, Michigan State University,
East Lansing, Michigan 48824, USA*

R. Schwengner

*Institut für Strahlenphysik, Helmholtz Zentrum Dresden Rossendorf,
01328 Dresden, Germany*

The enhancement observed below 2 MeV in the radiative strength function of nuclei near closed shells is explained by shell model calculations as M1 transitions between excited states. In the open-shell a change to a bimodal structure composed of the zero energy spike and a scissors resonance is found. The features are caused by realignment of high-j orbitals.

Keywords: radiative strength, shell model, high-j orbitals.

1. Introduction

Photonuclear reactions and the inverse radiative-capture reactions between nuclear states in the region of high excitation energy and large level density are of considerable interest in many applications. Radiative neutron capture, for example, plays a central role in the synthesis of the elements in various stellar environments, for next-generation nuclear technologies, and as the transmutation of long-lived nuclear waste.

A critical input to calculations of the reaction rates is the average strength of the cascade of γ -transitions de-exciting the nucleus, which is described by the radiative strength function. An increase of the dipole strength function below 3 MeV toward low γ -ray energy has recently been observed in nuclides in the mass range from $A \approx 40$ to 100. As an example,

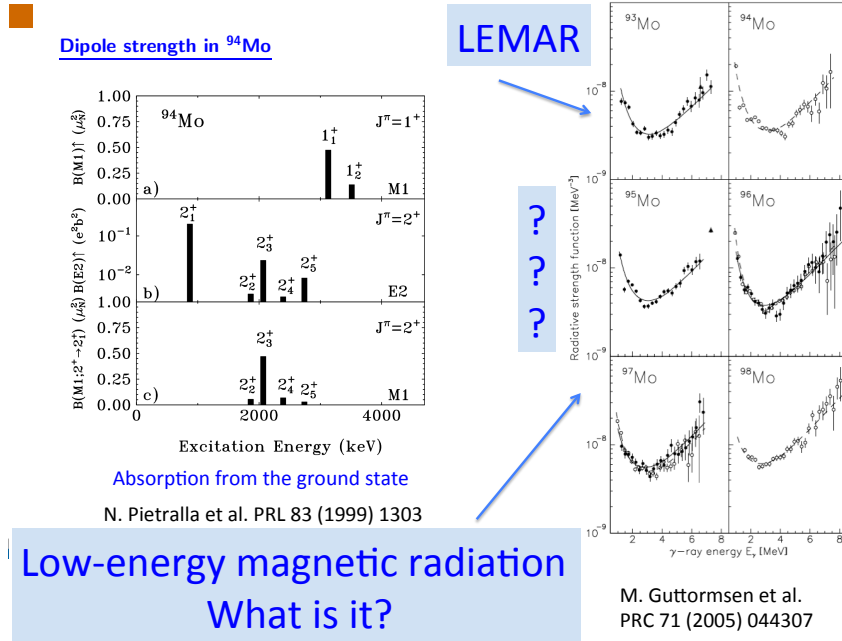


Fig. 1. (Color online) Left: Reduced absorption probabilities from the ground state by (γ, γ') experiments¹. Right: Strength function for γ de-excitation after the $(^3\text{He}, ^3\text{He}')$ reaction².

Fig. 1 shows the γ strength function obtained from $(^3\text{He}, ^3\text{He}')$ reactions on various Mo isotopes. The enhancement is not observed in the inverse process of absorbing γ -quanta by nuclei in the ground state. Only few discrete lines are found within the interval of the first 4 MeV. The question arises which is the origin of the radiation enhancement and how does it depend on the N and Z . Refs.^{3,4} showed that the low-energy enhancement may increase the neutron capture rate in the stellar r-process environment up to a factor 100-1000. The dominant dipole character of the low-energy strength was demonstrated in Ref.⁵ and an indication for an M1 character was discussed for the case of ^{60}Ni ⁶.

2. The LEMAR spike

Our Shell Model studies of the Mo isotopes explained the enhancement as Low Energy MAGnetic Radiation (LEMAR) generated by transitions between excited states few MeV above yrast⁷. The Shell Model calcula-

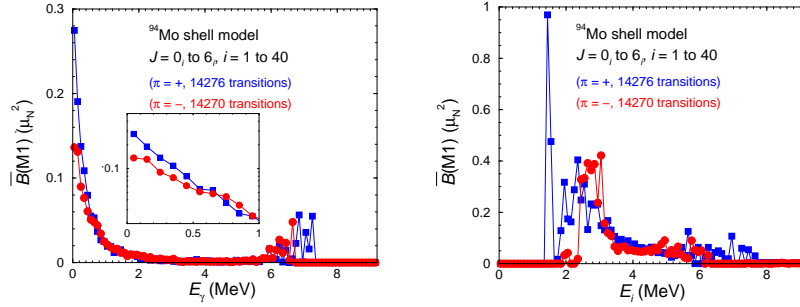


Fig. 2. (Color online) Left: Average $B(M1)$ values in 100 keV bins of transition energy calculated for positive-parity (blue squares) and negative-parity (red circles) states in ^{94}Mo . The inset shows the low-energy part in logarithmic scale. Right: Average $B(M1)$ values in 100 keV bins of excitation energy calculated for positive-parity (blue squares) and negative-parity (red circles) states in ^{94}Mo . From⁷.

tions included the active proton orbits $\pi(0f_{5/2}, 1p_{3/2}, 1p_{1/2}, 0g_{9/2})$ and the neutron orbits $\nu(0g_{9/2}, 1d_{5/2}, 0g_{7/2})$ relative to a ^{68}Ni core. A set of empirical matrix elements for the effective interaction and effective g -factors of $g_s^{\text{eff}} = 0.7g_s^{\text{free}}$ have been used. The calculations included states with spins from $J = 0$ to 6 for ^{90}Zr and ^{94}Mo and from $J = 1/2$ to $13/2$ for ^{95}Mo . For each spin the lowest 40 states were calculated. The reduced transition probabilities $B(M1)$ were calculated for all transitions from initial to final states with energies $E_f < E_i$ and spins $J_f = J_i, J_i \pm 1$. This resulted in more than 14000 $M1$ transitions for each parity $\pi = +$ and $\pi = -$, which were sorted into 100 keV bins according to their transition energy $E_\gamma = E_i - E_f$. The average $\overline{B}(M1, E_\gamma)$ value for one energy bin was obtained as the sum of all $B(M1)$ values divided by the number of transitions within this bin. The results for ^{94}Mo are shown in Fig. 2. The left panel demonstrates appearance of the LEMAR spike, which exponentially decreases with the transition energy E_γ . The exponential dependence on the transition energy is retained by the $M1$ strength functions, which are defined by the relation

$$f_{M1}(E_\gamma) = 16\pi/9(\hbar c)^{-3}\overline{B}(M1, E_\gamma)\rho(E_i), \quad (1)$$

where the level density at the initial state $\rho(E_i)$ is obtained from the Shell Model calculations.

As seen in the right panel of Fig. 2, LEMAR is generated by transition originating from states between 2 and 6 MeV. Inspecting the composition of initial and final states, we found large $B(M1)$ values for transitions

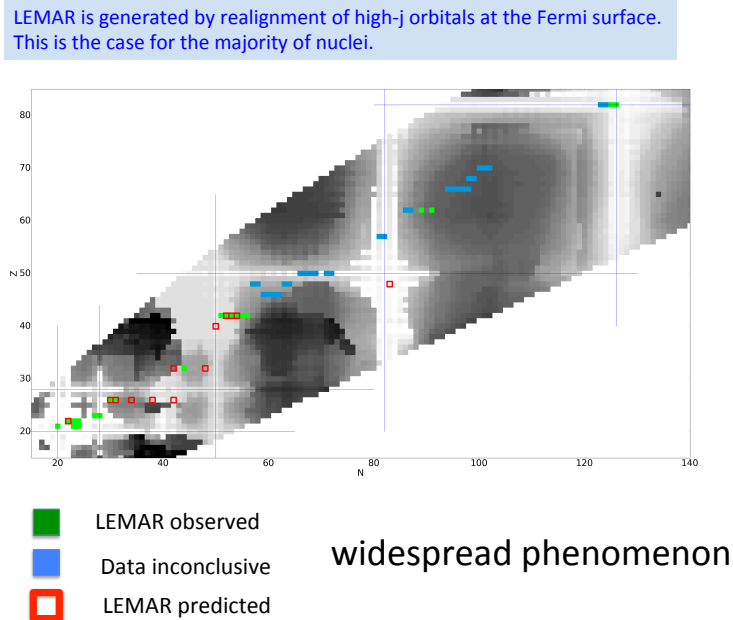


Fig. 3. (Color online) Experimental presence of the LEMAR spike and predictions by Shell Model calculations.

between states that contain a large component (up to about 50%) of the same configuration with broken pairs of both protons and neutrons in high- j orbits. The largest $M1$ matrix elements connect configurations with the spins of $g_{9/2}$ protons re-coupled with respect to $g_{9/2}$ neutrons to the total spin $J_f = J_i, J_i \pm 1$. These orbitals have large magnetic moments. Large $M1$ matrix elements connect configurations which differ by only the angular momentum projection of these high- j orbitals. Our Shell Model studies of $^{56,57}\text{Fe}^8$ and $^{60,64,68}\text{Fe}^9$ found also the LEMAR spike, which is generated by reorientation of $f_{7/2}$ proton holes and $g_{9/2}$ neutrons. High- j particle or hole orbitals with $j = l + 1/2$ have the largest magnetic moments. As they appear near the Fermi level all over the nuclear chart one expects that LEMAR spike is omnipresent as well.

The left panel of Fig. 4 shows the logarithm of the level density. At low energy the level density follows the constant temperature expression $\rho(E) = \rho_0 \exp(E/T)$. Above 4 MeV the level density is underestimated because of the truncation of the configuration space. The right panel demonstrates

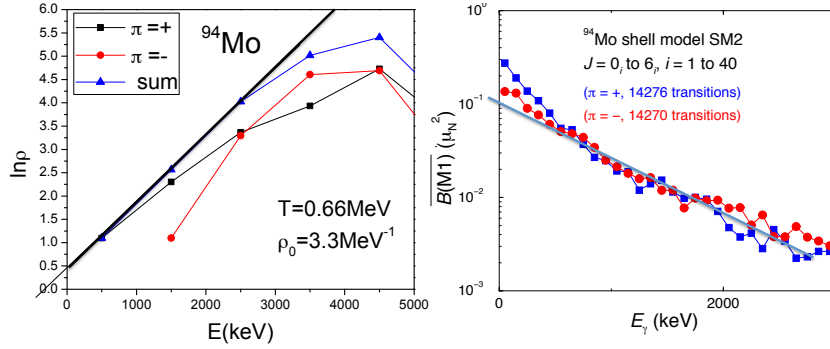


Fig. 4. (Color online) Left: Shell Model calculation⁷ of the level density (left) and average $B(M1)$ values of ^{94}Mo . The straight lines have the slope $\pm 1/T$, $T = 0.66 \text{ MeV}$.

that the exponential decrease of the LEMAR spike is consistent with T derived from the level density. For the Mo isotopes there is consistency between the value of $T \approx 0.8 \text{ MeV}$ derived from the experimental level densities¹⁰ and from the LEMAR spike of the γ strength functions². As illustrated by Fig. 7 below, the consistency also holds for the experimental level densities and γ strength functions of $^{151,153}\text{Sm}$.

3. Consequences of deformation and properties of the Scissors Resonance

In our Shell Model studies of $^{60,64,68}\text{Fe}^9$ we investigated the influence of quadrupole correlation on LEMAR. The calculations were carried out in the CA48PN model space with the CA48MH1 Hamiltonian using the code NuShellX@MSU. The model space included the $\pi(0f_{7/2}^{(6-t)}, 0f_{5/2}^t, 1p_{3/2}^t, 1p_{1/2}^t)$ proton orbits with $t = 0, 1, 2$, and the $\nu(0f_{5/2}^{n5}, 1p_{3/2}^{p3}, 1p_{1/2}^{p1}, 0g_{9/2}^{g9})$ neutron orbits. The calculations of M1 strengths were carried out in the same way as for the Mo isotopes. They included the lowest 40 states each with spins from $J_i, J_f = 0$ to 10, which resulted in more than 22000 M1 transitions for each parity. Effective g factors of $g_s^{\text{eff}} = 0.9g_s^{\text{free}}$ were applied.

The comparison with the experimental $B(E2, 2_1^+ \rightarrow 0_1^+)$ values in the Table included in Fig. 5 shows that the calculations reproduce the quadrupole collectivity in the considered isotopic chain, in particular the enhancement observed around $N = 40$. The respective experimental ratios

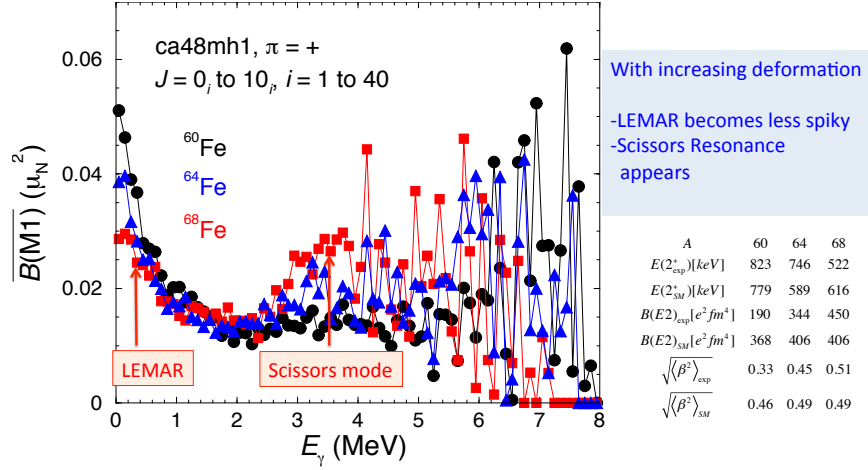


Fig. 5. (Color online) Calculated average $B(M1)$ values for the positive parity states in $^{60,64,68}\text{Fe}$. The table compares the calculated properties of the first 2^+ state with experiment.

$E(4^+)/E(2^+)=2.57, 2.36, 2.66$, which are well accounted for by the calculations $E(4^+)/E(2^+)=2.56, 2.68, 2.43$, indicate the transitional character of the ground state bands of all considered isotopes.

The comparison of the $\overline{B}(M1)(E_\gamma)$ values of the various isotopes shows that the shape of the distributions changes when going from $N = 34$, four neutrons above the closed shell, to $N = 42$, the middle of the fp shell. One observes a weakening of the LEMAR spike and the development of a bump in the range from about 2 to 5 MeV, which is most pronounced in ^{68}Fe . We interpret this bump as the Scissors Resonance (SR) built on excited states.

Fig. 6 shows the M1 strength functions for $^{60,68}\text{Fe}$, which were calculated using level densities from the Shell Model calculations. Like the average $\overline{B}(M1)$ values they develop the bimodal LEMAR-SR structure when going to the middle of the open shell. The integrated strength deduced from the strength functions below 5 MeV varies by only 8% at most from an average of $9.80 \mu_N^2$. The slight increase with N is attributed to the progressive occupation of the $g_{9/2}$ shell for $N = 34, 38, 42$. That is, the bimodal structure develops with increasing N by shifting strength from the LEMAR spike to the SR while the sum stays nearly constant.

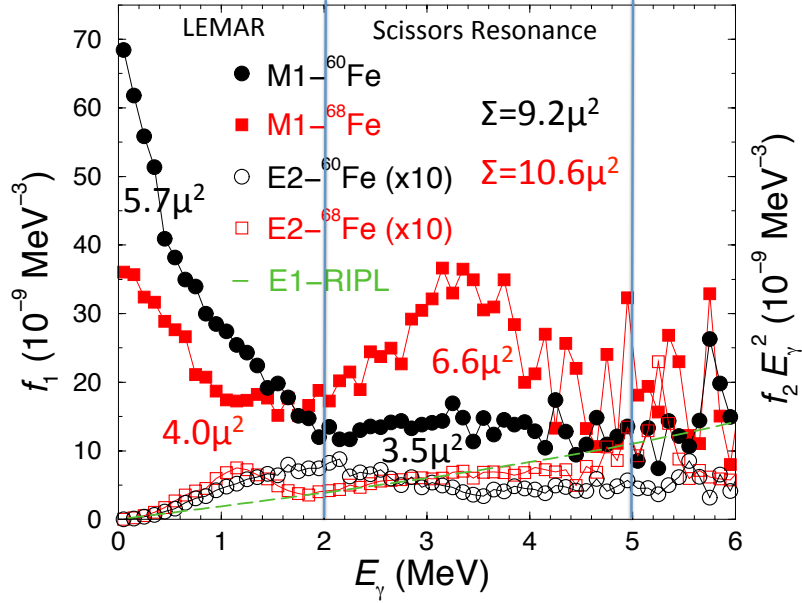


Fig. 6. (Color online) Calculated M1 strength functions (f_1) and E2 strength functions ($f_2 E_\gamma^2$) in $^{60,68}\text{Fe}$. Note the factor of 10 for E2. The numbers quote the integrated strength for the LEMAR spike ($\int_0^2 f_1(E)dE$) and the Scissors Resonance ($\int_2^5 f_1(E)dE$). The vertical lines indicate the respective integration regions. For ^{68}Fe the sum of the M1 strength from the ground state to all 1^+ states is $\sum B(M1, 0_1^+ \rightarrow 1^+) = 1.7\mu^2$.

For comparison, the standard E1 strength function with parameters taken from the RIPL data base and E2 strength functions f_2 obtained from the present calculations are also shown in Fig. 6. The latter were multiplied with E_γ^2 to be directly comparable with the dipole strength functions f_1 . The E2 strength $f_2 E_\gamma^2$ is more than one order of magnitude smaller and the E1 strength exceeds the M1 strength only at energies greater than 6 MeV.

The strength functions deduced by means of the Oslo method from high-resolution experiments by A. Simon *et al.*⁴ showed for the first time the LEMAR spike down to about $E_\gamma = 1$ MeV as well as a SR around 3 MeV in one nuclide. Fig. 7 displays the results together with a table of the properties of the 2^+ states of the neighbors, which demonstrate the well deformed nature of the nuclides. Thus we conclude that the bimodal LEMAR-SR structure is a general feature expected for all deformed nuclei.

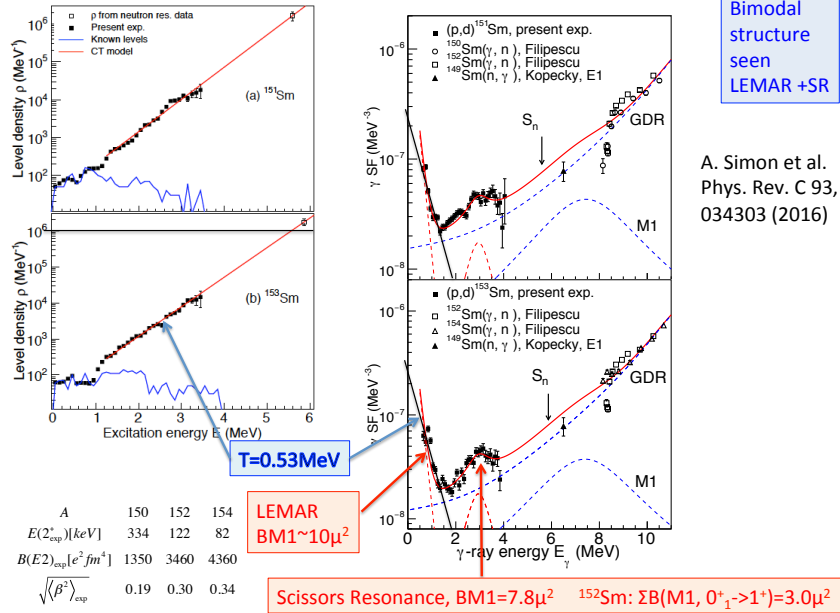


Fig. 7. (Color online) Experimental level densities (left) and γ strength functions (right) of $^{151,153}\text{Sm}$ measured and derived by means of the Oslo method⁴. The dashed lines show a fit of three Lorentzians (GDR, M1GR, SR) to the γ strength functions. The temperature T derived from the slope of the level density (left) is used to extrapolate the LEMAR spike to $E_\gamma = 0$. The sum of the M1 strength from the ground state to all 1^+ states is quoted at the bottom.

Fig. 8 illustrates how the development of the bimodal LEMAR-SR structure can be attributed to the onset of stable quadrupole deformation above the yrast line when entering the open shell. The mechanism causing large $B(M1)$ values is reorientation of the high- j single-particle angular momenta. Without deformation this occurs between the various configurations of the nucleons in an incompletely filled j -shell, $h_{11/2}$ in the example, which generates the LEMAR spike as suggested in Ref.⁷ and discussed above. The magnetic (m) substates of the high- j multiplet split with the onset of deformation. Reorientation occurs in two different ways. First, there are the real transitions between the m -substates. Particle-hole excitations of this type are known to generate the SR¹¹. As seen in Fig. 8, the splitting between the m -states corresponds to the position of the SR for $\varepsilon = 0.3$. Second, there are the virtual excitations from the occupied to

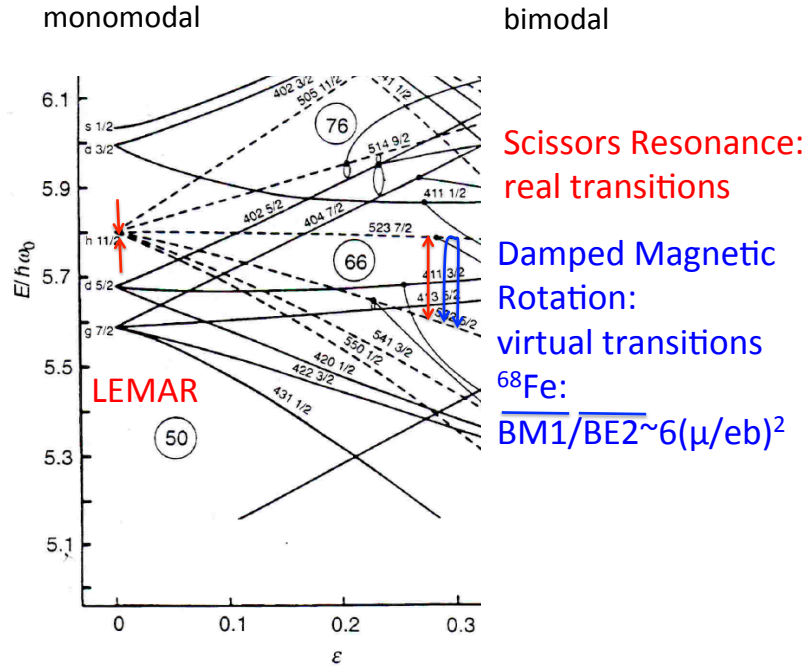


Fig. 8. (Color online) Transitions that generate the LEMAR spike and the Scissors Resonance. The energy scale is $\hbar\omega_0 = 7.7$ MeV for $A = 153$.

the empty m -states. These are known generating the rotational motion of deformed nuclei. Along a rotational band the angular momentum increases by a coherent gradual alignment of the spins of the nucleons in the deformed orbitals, which is described by the virtual particle-hole excitations between the m -states. As discussed in our paper⁹, the rotational coherence is only partially realized for the transition between the states several MeV above yrast. With increasing deformation, the LEMAR spike changes from incoherent thermal-like radiation to partially coherent rotational radiation. The onset of damped rotation can be seen in the E2 strength function for ^{68}Fe shown in Fig. 6. The bump at 1.2 MeV is generated by stretched E2 transitions with $E_\gamma = 2I/\mathcal{J}$, where $\mathcal{J} \approx 12 \text{ MeV}^{-1}$ is close to the rigid body moment of inertia. The LEMAR spike of ^{68}Fe in Figs. 5 and 6 deviates from the exponential form at the lowest energies, which can be traced back to the presence of an rotational component with $E_\gamma = I/\mathcal{J}$.

In (γ, γ') experiments 1^+ states are excited from the ground state that

group to the SR in deformed nuclei. In the case of ^{68}Fe the summed strength of these transitions is calculated to be $\sum B(M1, 0_1^+ \rightarrow 1^+) = 1.7 \mu^2$. The integral of the strength function between 2 and 5 MeV amounts to $6.6 \mu^2$, which is three and a half times larger (see Fig. 6). From their experiment on $^{151,153}\text{Sm}$, Ref. ⁴ assigned an integrated strength of $7.8 \mu^2$ to the SR, which is two and a half times larger than the summed strength of the excitation of the SR from the ground state of ^{152}Sm (see Fig. 7). A similar enhancement of the SR strength in the γ decay as compared with the excitation of the SR from the ground state by (γ, γ') experiments has been reported before (see Ref. ⁴ for references).

The origin of the enhancement of the transition strength is an increase of transitions from excited states as compared to $0_1^+ \rightarrow 1^+$. For example in ^{68}Fe , $\sum B(M1, 0_2^+ \rightarrow 1^+) = 3.4\mu^2$. We attribute the larger summed strengths between excited states to a suppression of the pair correlations with increasing excitation energy, i.e. the thermal quenching of pairing. Pair correlations tend to couple the high- j orbits to zero spin, which obstructs the reorientation that generates the M1 radiation.

S. F. acknowledges support by the DOE Grant DE-FG02-95ER4093, B. A. B. support by the NSF Grant PHY-1404442, and all authors acknowledge the importance of the ECT* workshop on "Statistical properties of nuclei", July 11 - 15, 2016, for advancing this research.

References

1. N. Pietralla *et al.*, Phys. Rev. Lett. **83**, 1303 (1999).
2. M. Guttormsen *et al.*, Phys. Rev. C **71**, 044307 (2005).
3. A. C. Larsen and S. Goriely, Phys. Rev. C **82**, 014318 (2010).
4. A. Simon *et al.*, Phys. Rev. C **93**, 034303 (2016).
5. A. C. Larsen *et al.*, Phys. Rev. Lett. **111**, 242504 (2013).
6. A. Voinov *et al.*, Phys. Rev. C **81**, 024319 (2010).
7. R. Schwengner, S. Frauendorf, and A. C. Larsen, Phys. Rev. Lett. **111**, 232504 (2013).
8. B. Alex Brown and A. C. Larsen, Phys. Rev. Lett. **113**, 252502 (2014).
9. R. Schwengner, S. Frauendorf, A. Brown, Phys. Rev. Lett. in print.
10. R. Chankova *et al.*, Phys. Rev. C **73**, 034311 (2006).
11. I. Hamamoto and S. Åberg, Phys. Lett. B **145**, 164 (1984).